JBC ARTICLE

Sensitive quantification of α-glucans in mouse tissues, cell cultures, and human cerebrospinal fluid

Received for publication, June 30, 2020, and in revised form, August 4, 2020 Published, Papers in Press, August 13, 2020, DOI 10.1074/jbc.RA120.015061

Silvia Nitschke[1], Sara Petković[2], Saija Ahonen[2], Berge A. Minassian[1,2], and Felix Nitschke[1,*]

From the [1]Departments of Pediatrics and Biochemistry, University of Texas Southwestern Medical Center, Dallas, Texas and the [2]Program in Genetics and Genome Biology, The Hospital for Sick Children Research Institute, Toronto, Ontario, Canada

Edited by Gerald W. Hart

The soluble α-polyglucan glycogen is a central metabolite enabling transient glucose storage to suit cellular energy needs. Glycogen storage diseases (GSDs) comprise over 15 entities caused by generalized or tissue-specific defects in enzymes of glycogen metabolism. In several, *e.g.* in Lafora disease caused by the absence of the glycogen phosphatase laforin or its interacting partner malin, degradation-resistant abnormally structured insoluble glycogen accumulates. Sensitive quantification methods for soluble and insoluble glycogen are critical to research, including therapeutic studies, in such diseases. This paper establishes methodological advancements relevant to glycogen metabolism investigations generally, and GSDs. Introducing a pre-extraction incubation method, we measure degradation-resistant glycogen in as little as 30 mg of skeletal muscle or a single hippocampus from Lafora disease mouse models. The digestion-resistant glycogen correlates with the disease-pathogenic insoluble glycogen and can readily be detected in very young mice where glycogen accumulation has just begun. Second, we establish a high-sensitivity glucose assay with detection of ATP depletion, enabling 1) quantification of α-glucans in cell culture using a medium-throughput assay suitable for assessment of candidate glycogen synthesis inhibitors, and 2) discovery of α-glucan material in healthy human cerebrospinal fluid, establishing a novel methodological platform for biomarker analyses in Lafora disease and other GSDs.

Glycogen, a branched polymer of glucose, is a central part of cellular metabolism in many animal tissues, such as liver, muscle, brain, kidney, adipose tissue, and heart (1). Although the exact role and quantity of glycogen is tissue-specific, in general its function is to store glucose in an enzymatically accessible macromolecule inside of cells and to release it when metabolically required (2).

De novo synthesis of the α-glucan glycogen is usually initiated in the cytosol by glycogenin (3), which first autoglycosylates and then elongates the nascent glucan chain forming α1,4-interglucose linkages, using UDP-glucose as a glucosyl donor. Chain elongation is then continued by glycogen synthase (1). As longer unbranched glucan chains form double helices and precipitate (4), glycogen branching enzyme is required to introduce α1,6-linkages (branching points) and maintain solubility. The concerted action of chain elongation and branching results in a relatively compact yet water-soluble glycogen molecule that can reach sizes of ~55,000 glucosyl units. Glycogen degradation is mediated in the cytosol by glycogen phosphorylase and debranching enzyme, generating largely glucose 1-phosphate, and in the lysosome by α-glucosidase, generating mostly glucose (1).

Genetic defects in enzymes with a role in glycogen metabolism are responsible for glycogen storage diseases (GSD) and emphasize the centrality of a functioning glycogen metabolism. In some GSDs, enzymes directly involved in glycogen synthesis or its degradation, as the ones described above, can be affected. Other GSDs are caused by deficiencies in enzymes that mediate pathways immediately feeding into glycogen synthesis, or by lack or impairment of enzymes required for downstream processing of glycogen degradation products (5). Consequently, most of the GSDs are characterized by an abnormal quantity of glycogen in the affected tissue (2). In some cases, the quality of glycogen is also affected: in various tissues from patients of Andersen disease (6), Lafora disease (LD) (7), AMP-activated protein kinase deficiency (8), and phosphofructokinase deficiency (9), an insoluble form of glycogen accumulates in the form of so-called polyglucosan bodies, which appear to be metabolically inert. For LD, caused by mutations in either *EPM2A* (laforin) or *NHLRC1* (*EPM2B*, malin), it has been shown that such aggregates of insoluble glycogen are the driver of the disease progression (10). Insoluble brain glycogen has also been described as corpora amylacea in association with aging (11).

Appropriate methods for quantification of soluble and insoluble glycogen are essential tools in the study of glycogen metabolism in health and disease. Recently, soluble and insoluble glycogen was isolated from skeletal muscle of three different GSD mouse models with polyglucosan body accumulation (12). The methodology was designed to enable structural analysis of the glycogen fractions. For sole quantification of soluble and insoluble glycogen, especially in younger mice with less progressed glycogen accumulation, simpler methods requiring less tissue are favorable. Furthermore, sensitive detection of glycogen in cultured cells is prerequisite for the characterization of candidate therapeutics targeting, for instance, glycogen synthase in GSDs with glycogen overproduction (13). The detection of CSF biomarkers in neurodegenerative diseases is common (14). In urine of Pompe disease (GSDII) patients glycogen degradation products have been found abnormally high (15, 16). GSD-related changes in brain glycogen, *e.g.* in LD, suggest the sensitive detection of glycogen or glycogen-derived glucose as a viable biomarker in cerebrospinal fluid (CSF). The work in this paper describes methodological advances on all these fronts.

* For correspondence: Felix Nitschke, felix.nitschke@utsouthwestern.edu.

Generally, glycogen can be detected by immunohistochemistry using periodic acid-Schiff stain (PAS). The presence of large PAS-positive aggregates in skin biopsies of suspected LD cases has long been decisive in the diagnosis of the disease (10, 17). Quantitative comparison between PAS-stained samples requires strictly controlled tissue treatment and staining procedures that can be achieved in animal studies but hardly in a clinical setting.

Immunofluorescence detection of glycogen utilizes a glycogen-directed antibody (18) or other glycogen-binding proteins that can be labeled by secondary antibodies (19). This methodology is generally restricted to cell culture experiments. Also, immunofluorescence-based methods mostly focus on the localization of the antigen and are, unless extensively standardized, considered at best semiquantitative (20).

Methods for more precise glycogen quantification in animal tissue usually comprise the steps: 1) tissue lysis and glycogen extraction, 2) glycogen degradation, and 3) glucose determination. Extraction from pulverized tissue in hot 30% potassium hydroxide has been widely used for glycogen quantification (21–23). Other extraction procedures include homogenization in cold 10% TCA (24–26) or in Tris-based glycogen isolation buffer (12, 27). Extraction in a suitable buffer allows separation of soluble and insoluble glycogen, followed by glycogen quantification without further purification of the glycogen by repeated ethanol precipitations (12), which are otherwise required to remove excess amounts of potassium hydroxide or TCA. Repeated precipitation of glycogen also removes low-molecular compounds such as blood-derived glucose (28), which can interfere with the determination of glycogen-derived glucose. Hydrolysis of virtually all interglucose linkages in glycogen can be achieved by amylolytic treatment using amyloglucosidase, either alone (12, 21, 27) or in combination with amylase (25). Hydrolysis in hot 0.7-1 M hydrochloric acid or 2 M TFA (29–31) can also be utilized to degrade glycogen prior to glucose quantification.

If glucose is quantified in glycogen hydrolysates after several rounds of ethanol precipitation, the detected amount of glucose is considered to represent the glycogen quantity, as the amount of free (*i.e.* nonglycogen-derived) glucose is negligible (22, 23). Beside macromolecular glycogen, tissue extracts that have not undergone repeated ethanol precipitation contain free glucose (*e.g.* from blood). In such samples it is therefore crucial to determine the amount of free glucose present before glycogen hydrolysis. Logically, the relative contribution of free glucose to post-hydrolysis glucose (free and glycogen-bound glucose) is higher in tissues with low glycogen amount, such as brain or heart (22, 23). The difference between glucose contents determined with and without glycogen degradation is the total amount of α-glucan, a proxy for glycogen, which includes glycogen but possibly also smaller α-glucan chains that would be excluded by ethanol precipitations (32).

The sensitivity of the entire glycogen quantification procedure is greatly dependent on the sensitivity of the glucose assay used after glycogen degradation. Simple enzymatic assays detect products of enzymatic glucose conversion. For instance, spectrophotometrically detectable NAD(P)H is generated during the conversions of glucose by hexokinase (HK) and glucose-6-phosphate dehydrogenase (G6PDH) in the presence of ATP and NAD(P) (12, 23, 25). Alternatively, various dyes can be detected after reaction with hydrogen peroxide as generated by glucose oxidase (27, 33). Most of these assays are suitable for glycogen determination in many animal tissues when sufficient tissue is available. If the glycogen content is very low or the amount of available tissue is limited, more sensitive methods for glucose determination are advantageous.

ATP can be quantified with very high sensitivity when utilizing luminescence detection during the ATP-dependent oxidation of luminol to oxiluminol as mediated by firefly luciferase (34). ATP detection is now widely used for sensitive cell viability analyses (35, 36).

In this paper three methodological advancements are described. First, a simple pre-extraction incubation step is demonstrated to reliably reveal an inert (degradation resistant) fraction of glycogen in skeletal muscle (5 months old) and hippocampus (3 months old) of mouse models of LD. Second, a glucose assay was established that detects glucose-dependent ATP depletion utilizing firefly luciferase-mediated generation of luminescence. Third, a method is presented that enables the detection of minute amounts of α-glucan material in commercial samples of human CSF.

Results and discussion

Quantification of inert α-glucans in muscle of LD mice

We aimed to develop a simple method that allows quantification of the soluble and insoluble portion of glycogen in small amounts of mouse tissue. We tested whether pre-extraction exposure to physiological temperatures of muscle tissue will lead to the removal of soluble glycogen, whereas insoluble will remain. Ground skeletal muscle from 5-month–old WT and malin-deficient mice (*Epm2b*$^{-/-}$, mouse model of LD) was pooled from 3 animals each and divided into equal aliquots. These were incubated at 37 °C for various times between 0 and 6 h before they underwent glycogen extraction and quantification as illustrated in Fig. 1*A*. In both WT and *Epm2b*$^{-/-}$ samples glycogen degraded rapidly, showing reduction of glycogen levels by over 90% within 15 min of pre-extraction incubation. After about 1 h the content of remaining glycogen stabilized in WT and *Epm2b*$^{-/-}$ samples. However, whereas there was almost no glycogen remaining in WT, the content in the mutant tissue stabilized at a consistently higher level and remained essentially unchanged within the following 5 h of incubation (Fig. 1*B*). Subsequently, muscle tissue from 6 individual mice per genotype was subjected to 0 and 1.5 h pre-extraction incubation prior to glycogen quantification. In both genotypes the total glycogen content (0 h) was on average between 15 and 16 μmol of glucosyl units/g of fresh weight. Pre-extraction incubation led to strongly reduced glycogen contents in all mice. The WT and mutant tissues contained on average 0.08 and 1.26 μmol of glucosyl units/g of fresh weight, respectively. These values account for about 0.5 and 7.6% of the average total glycogen in the respective genotypes (Fig. 1*C*).

The average total glycogen content measured in muscle of 5-month–old WT and *Epm2b*$^{-/-}$ mice is within the range of what has previously been published for skeletal muscle in WT

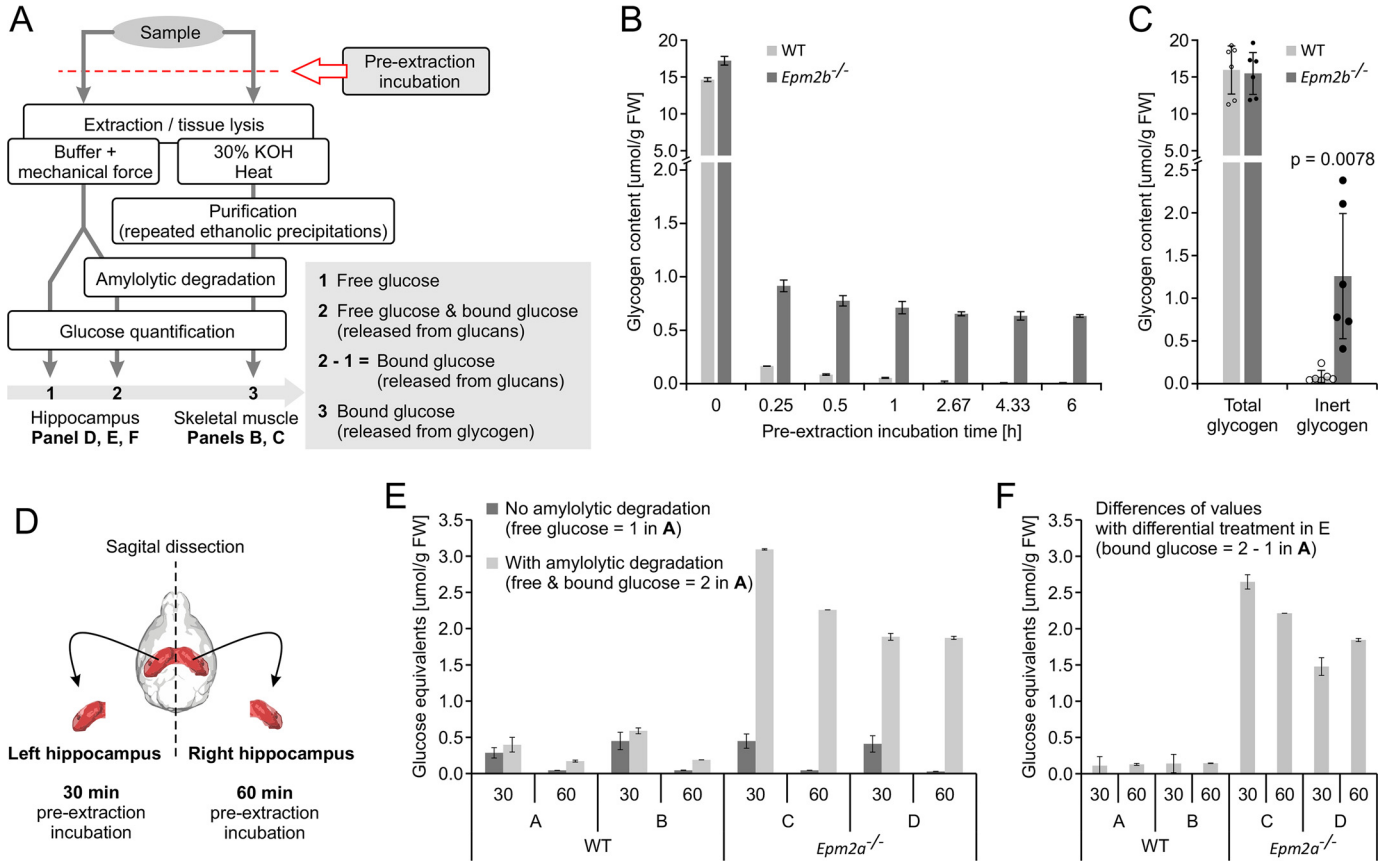

Figure 1. Determination of inert α-glucans in mouse muscle and hippocampus. *A,* schematic, illustrating the procedure of glucan quantification in biological material. Depending on the type of extraction and tissue lysis, ethanol precipitations or additional controls for amylolytic degradation become necessary. The *red line* indicates at which step during the procedure an additional incubation step was performed in experiments referred to in *B* to *F*. *B,* glycogen content in aliquots of pooled skeletal muscle tissue from 5-month–old WT and *Epm2b*$^{-/-}$ mice. Aliquots were subjected to pre-extraction incubation at 37 °C for the indicated amount of time and glycogen determination proceeded as indicated in *A* for skeletal muscle. *Error bars* represent the mean absolute deviation between two identically treated tissue aliquots. *C,* total and inert glycogen in muscle of 5-month–old WT and *Epm2b*$^{-/-}$ mice. Inert glycogen was determined as the residual glycogen present after 1.5 h pre-extraction incubation at 37 °C. Average of 6 individual mice per group, with *error bars* representing S.D. and *p* value derived from Welch's two-tailed *t* test. *D,* schematic, illustrating the use of the hippocampi from both mouse brain hemispheres for the determination of inert α-glucan material in 30-month–old WT and *Epm2a*$^{-/-}$ mice as referred to in *E* and *F*. *E* and *F,* determination of inert glucan content in the hippocampi of two WT (*A* and *B*) and two *Epm2a*$^{-/-}$ mice (*C* and *D*). Hippocampi were subjected to pre-extraction incubation for either 30 (left hippocampi) or 60 min (right hippocampi), and glucan determination proceeded as indicated in *A* for hippocampus. Depending on amylolytic treatment, free glucose or both free glucose and glucan-bound glucose were quantified, respectively (*E*). Glucan-bound glucose was calculated as the difference of values determined with and without amylolytic treatment (*F*). Averages of independent glucose determinations are depicted with *error bars* representing mean absolute deviation of two technical replicates (*E*). Upon calculation of differences, mean absolute deviations were adjusted to account for variances of the two independently determined glucose quantities used for the calculation (*F*, see "Statistical analysis").

mice (12, 22, 23, 31, 37, 38) with the exception of a recent publication that, using GC/MS following a novel extraction protocol, demonstrated muscle glycogen contents less than 10% of all previous findings (26). Glycogen accumulation in muscle of 9-12–month–old LD mice was previously clearly detected, but changes in total muscle glycogen content were mostly undetectable in mice younger than 5 months (22, 37). Pre-extraction incubation of muscle tissue as established here reveals the presence of an abnormal kind of glycogen in skeletal muscle of LD mice already at 5 months of age. This abnormal glycogen is absent in WT mice and seems to be inert to the degradation process that removes essentially all WT glycogen during pre-extraction incubation. This degradation is expected to be mediated by endogenous enzymes that reactivate when the tissue sample warms up. The only enzymes known to degrade glycogen *in vivo* are glycogen phosphorylase and the lysosomal α-glucosidase, which are expressed in essentially all glycogen storing tissues. Phosphorylase has been shown stimulated under hypoxic and hypoglycemic conditions (39, 40). Both conditions can safely be assumed fulfilled in a tissue piece cut off from blood circulation. During pre-extraction incubation of powdered muscle tissue blood-derived pancreatic amylase and lysosomal α-glucosidase could certainly contribute to glycogen degradation, as they may gain access to cytosolic components due to the breaking of cells and compartments during tissue pulverization. Determination of inert muscle glycogen can be done with less than 30 mg of muscle tissue and will provide unprecedented insight when polyglucosan accumulation is studied in models of GSDs at a younger age, such as in investigations into disease onset or early intervention.

Quantification of inert α-glucans in hippocampi of LD mice

Historically, muscle and brain are the tissues mainly studied in LD. In addition to muscle we examined the presence of inert glycogen in brain tissue, in particular the hippocampus. We

used the alternative mouse model of LD (*Epm2a*$^{-/-}$), which is indistinguishable from *Epm2b*$^{-/-}$ mice with respect to accumulation of insoluble glycogen in the brain (23). Hippocampi of 3-month–old *Epm2a*$^{-/-}$ and WT mice were subjected to pre-extraction incubation and subsequent glycogen quantification. Hippocampi were dissected from each hemisphere and frozen in liquid nitrogen separately. From each mouse one hippocampus was incubated for 30 min, the other for 60 min (Fig. 1*D*). The brain tissue was incubated at 25 °C as we indicated that room temperature exposure of brains suffices to cause a substantial decrease in brain glycogen, such as when dissection and freezing of brains was delayed after cervical dislocation of mice (data not shown). After pre-extraction incubation glycogen was extracted by homogenization in a buffer that provided favorable conditions for the subsequent amylolytic glycogen degradation. Glucose was determined using a conventional G6PDH/HK-based glucose assay before (free glucose) and after amylolysis (free glucose and that bound to α-glucans) (Fig. 1*A*). The amount of free glucose is similar in identically treated WT and mutant hippocampi, but it seems to be consistently reduced when pre-extraction incubation is extended to 60 min. The amount of post-amylolysis glucose tends to be greater than that of free glucose in all hippocampi. However, this effect is much more pronounced in *Epm2a*$^{-/-}$ compared with WT, where the post-amylolysis content is mostly driven by the amount of free glucose (Fig. 1*E*). The differences of pre- and post-amylolysis glucose contents define the samples' α-glucan content, which is clearly increased in the mutant hippocampi but largely unaffected by an extended incubation time (Fig. 1*F*).

The results demonstrate that *Epm2a*$^{-/-}$ hippocampi contain inert α-glucan material, which is unaffected by the degradation processes that lead to the near-complete depletion of α-glucans in WT hippocampi. It is expected that glycogenolysis in intact brain tissue is mostly phosphorylase-driven (see above). The differences between the WT and *Epm2a*$^{-/-}$ amounts are in line with accumulated glycogen previously described in 3-month–old LD mice brains (22, 37), further validating that the inert glucans we measured directly correspond with the abnormal glycogen that accumulates in LD. As in muscle, a pre-extraction incubation as devised removes all soluble and non-inert glycogen, revealing a very robust difference between diseased and WT animals already at a young age. As studies in young mice can be completed faster and therefore present a smaller financial burden, this method will be beneficial in studies assessing efficacy of therapeutic approaches for prevention or removal of insoluble brain glycogen, such as in LD (10, 31) or adult polyglucosan body disease (41). The sensitivity of the described method is sufficient to determine inert α-glucans in pieces of mouse brain weighing less than 20 mg, *e.g.* one hippocampus.

As the enzymatic processes leading to glycogen degradation are expected to be similar in any dissected tissues, we anticipate that the method described here can be used to quantify "inert" glycogen in tissues other than brain and skeletal muscle or in other mouse models. However, it is advisable to perform adequate control experiments for confirmation in each tissue and mouse line.

Increased sensitivity of glucose quantification by bioluminescence detection of ATP depletion

A sensitive method for glucose quantification allows the use of very low source material for α-glucan/glycogen quantification. Previously described enzymatic assays require a minimum of 500-1000 pmol of glucose/assay for reliable detection. ATP can be quantified by detection of bioluminescence generated in the firefly luciferase-mediated reaction of luminol to oxiluminol, the sensitivity of which exceeds the detection for instance of NADPH by more than 3 orders of magnitude (34, 42).

The principle of a glucose-dependent ATP depletion assay with bioluminescence detection is illustrated in Fig. 2*A*. Authentic glucose standards were subjected to a two-step protocol: 1) the HK reaction was conducted with a concentration of ATP that exceeds the highest glucose standard, 2) after completion of the HK reaction and dilution, an aliquot was added to a commercial ATP determination kit solution, and bioluminescence was detected with a luminescence microplate reader. A strictly linear negative correlation between glucose amount and relative luminescence units was observed in the range of 4 to 140 pmol of glucose in the HK reaction mix (Fig. 2*B*). In a different experiment glucose standards in the range of 1 to 10 pmol were subjected to the assay and also yielded in a strong analyte:signal correlation, which was best described by a second degree polynomial regression (Fig. 2*C*). In both experiments deviation between technical replicates was extremely small. These data show the capability of the assay to reproducibly and sensitively detect glucose at quantities that are up to 3 orders of magnitude lower than previously described enzymatic assays.

Quantification of α-glucans in HEK293 cells cultured in 96-well format

Monitoring glycogen synthesis in human cell culture is crucial in any therapeutic study targeting central enzymes of glycogen metabolism. For instance, glycogen synthase has been identified a therapeutic target in LD (13, 43, 44) and adult polyglucosan body disease (41).

An assay devised to quantify α-glucans in HEK293 cells cultured in a medium throughput format (96 well) has been established and employed in an experimental setup as illustrated in Fig. 2*D*. Cells seeded into 96-well–plates, were starved by exposure to glucose-free medium for 24 h. Subsequently the medium glucose concentration was changed back to 25 mM and "re-feeding" occurred for a variable amount of time. After that, cells were resuspended in cold water and aliquots were taken for the quantification of protein and glucans (utilizing the glucose-dependent ATP depletion assay). The glucan content changes in correlation with the re-feeding time. After 24 h of glucose deprivation cellular glucan content is close to 0, and it increases in a largely linear fashion within 6 h of re-feeding. Glucan contents after 8 h of re-feeding are indistinguishable from that in cells that did not undergo starvation (Fig. 2*E*). These results are in essence corresponding to previous data shown in Rat-1 fibroblasts (19). However, compared with the previous study, the statistical resolution is very high. Changes of cellular glycogen content within as low as 1 h are statistically significant attesting to the precision of the assay. Also, the cell

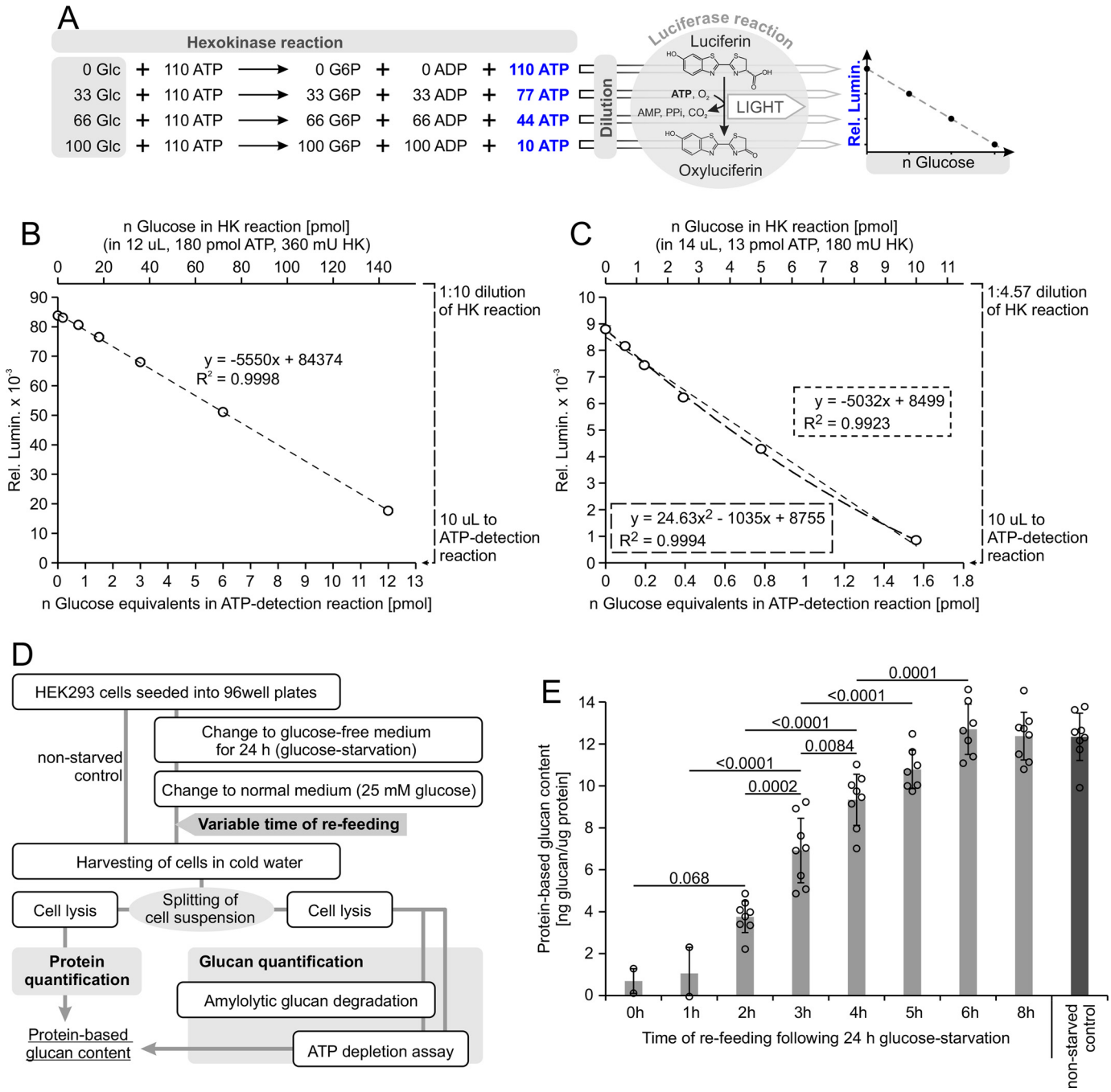

Figure 2. Sensitive detection of α-glucans using an ATP depletion assay. *A,* simplified numeric illustration of a glucose assay with detection of ATP depletion. Glucose (*Glc*) is converted to glucose 6-phosphate (*G6P*) in the presence of hexokinase and ATP. In the subsequent luciferase reaction remaining ATP correlates positively with relative luminescence (*Rel. Lumin.*), which itself negatively correlates with the glucose concentration. Note that the highest detectable glucose concentration is lower than the ATP start concentration. The high sensitivity of the ATP-dependent luminescence detection can require dilution after the hexokinase reaction. *B* and *C,* authentic glucose standards with ATP-depletion detection in two sensitivity ranges. The *top* axis denotes the amount of glucose added to the HK reaction (with total reaction volume, ATP start concentration, and HK activity given). The *bottom* axis denotes amounts of glucose equivalents (*i.e.* ATP-depletion units) that are subjected to the luciferase reaction after dilution of the HK reaction. Values are averages of relative luminescence in two technical replicates with mean absolute deviation represented by *error bars* (note, these are too small to be graphically discernible). Linear and/or polynomial regression curves show the correlation of glucose amount subjected to the assays and detected luminescence. *D,* schematic of the experimental setup to measure α-glucan material in HEK293 cells in 96-well format during different stages of re-feeding after glucose deprivation using the ATP depletion assay for glucose detection. Glucan material was quantified as defined by "bound glucose" in Fig. 1*A*, *i.e.* the portion of total glucosyl content that is amylolytically sensitive. Glucan amounts were normalized to the protein content of the same cell sample. *E,* HEK293 α-glucans were depleted by glucose deprivation for 24 h and resynthesized within 8 h of glucose re-feeding. Glucan content as normalized to total protein (protein-based glucan content) was determined as described in *D*. Values represent averages of cells from typically 7 or 8 individual but identically treated wells. *Error bars* represent S.D. Numeric values are select *p* values of one-way analysis of variance with Tukey post hoc tests.

number required for glucan quantification derived from a >80-fold smaller growth area. This facilitates the use of multiple well replicates, which is essential to reliably and quantitatively assess potential therapeutic effects on glycogen synthesis. By re-feeding in the presence of potential glycogen synthase inhibitors and α-glucan quantification after a defined amount of time, this assay could be readily adapted to assess the therapeutic potential of small molecule inhibitors with medium throughput efficiency.

Purification and detection of α-glucans in human CSF

Glycogen-derived glucan material could serve as a biomarker in studies of several GSDs. In this study human CSF was obtained from BioIVT, a commercial provider of biological specimen, and analyzed with respect to the presence of α-glucans.

For initial experiments CSF was pooled from several individuals. For that, the samples underwent heat denaturation to avoid degradation of potentially existing α-glucan chains by amylolytic enzymes present in CSF (45) and subsequent concentration by freeze-drying. At first free and glucan-derived (bound) glucose in the pooled CSF sample were determined using a standard enzymatic glucose assay with or without prior amylolysis. The free glucose content in the pooled CSF was around 2 mM, which is consistent with previous findings demonstrating that blood and CSF glucose levels are closely related (46). Amylolytic treatment of the pooled CSF sample did not reveal a detectable increase in glucose content (Fig. 3*A*), indicating that, if present at all, α-glucan–derived glucose concentrations in the CSF must be negligibly low compared with free glucose.

In an attempt to remove the vast majority of the free glucose, aliquots of the pooled CSF were subjected to repeated precipitation in 90% ethanol. Although glycogen is commonly and quantitatively precipitated at 67% ethanol (47, 48), a higher concentration was chosen to preserve putative smaller glycogen-derived α-glucan chains. During the repeated precipitation the recovery of glucose in each ethanolic supernatant was monitored, revealing the effective removal of usually more than 90% of glucose in each round of precipitation (Fig. 3*B*) and resulting in free glucose content around 50 nM after 4 rounds. After free glucose had been reduced by a factor of at least 4×10^5, amylolytic treatment revealed a noticeable increase in glucose, indicating the presence of 70 nM α-glucan–derived glucosyl residues in the pooled CSF sample. When precipitation had been conducted after spiking the pooled CSF with commercial linear α-glucans (also called oligo-maltodextrins), the amylolytic treatment yielded substantially more glucose without affecting the free glucose levels. This indicates that the precipitations preserved linear α-glucans and that they can be detected if present (Fig. 3*C*).

It has been shown that under the precipitation conditions applied here (90% ethanol, 4 °C) linear α-glucans up to a degree of polymerization (DP, chain length) of 7 remain soluble (32). The chain length pattern of the commercial oligo-maltodextrin preparation has been analyzed by high performance anion exchange chromatography with pulsed amperometric detection (HPAEC-PAD). A cumulative weight distribution, which assumes equal molar detection of all chain lengths, would explain a loss of about 20% of the glucosyl units in the maltodextrin mixture during the precipitation procedure, *i.e.* those chains shorter than DP 8 (Fig. 3*D*). Recovery of maltodextrin has been examined during the precipitations in the absence or presence of pooled CSF or authentic glucose, equivalent to amounts in CSF (Fig. 3*E*). Precipitation of maltodextrin alone or with authentic glucose led to a recovery of around 60% of maltodextrin glucosyl units. 50% were recovered when precipitated in the presence of pooled CSF. The discrepancy between the theoretically and experimentally determined maltodextrin losses can be explained by the fact that in HPAEC-PAD chromatograms detector response per chain increases with chain length (49, 50), which means detection of long chains is more sensitive. This results in a relative underrepresentation of the shorter chains in the cumulative weight distribution and likely to an underestimation of the impact of a potential loss of glucan chains DP 1 to 7. When the cumulative weight distribution of maltodextrin was adjusted for the differential sensitivity of detection of different chain lengths (using the model of Koch *et al.* (50)) the DPs 1 to 7 account for around 36% of the maltodextrin weight (Fig. 3*D*), which is in line with the loss we observed in our maltodextrin recovery experiment. The observed loss of maltodextrins during precipitation is therefore considered within the expected range.

Quantification of α-glucans in independent human CSF samples

α-Glucan content was subsequently quantified in independent human CSF samples to estimate biological variation. A procedure was established that requires 0.5-1 ml of CSF and utilizes the very sensitive ATP depletion assay for glucose determination after amylolytic treatment in the presence or absence of an internal standard of commercial glycogen (Fig. 3*F*). In each of the individual samples even after 4 rounds of precipitation free glucose accounted for 50–80% of the total glucosyl content (Fig. 3*G*). However, amylolysis consistently released additional glucose in all samples indicating the presence of α-glucans in all analyzed samples. Spiking of the CSF with a defined amount of commercial glycogen resulted in a uniform increase of glucose released by amylolysis. The concentration of α-glucan in human CSF was calculated from the difference of glucose contents determined with and without amylolysis in 9 individual samples (Fig. 3*H*). It ranges from 50 to 300 nM, the average being 133 ± 70 nM (S.D.). Upon passing the Kolmogorov-Smirnov test for normality ($p = 0.092$) a two-tailed one-sample *t* test was performed and attested that the average is significantly different from 0.0 ($p = 0.00046$).

These results demonstrate the presence of α-glucan chains in human CSF. The concentration of glucan-derived glucose is more than 5 orders of magnitude below that of free CSF glucose. Investigations into the structure and origin of the α-glucans have not been within the scope of this study. However, the methodology of their discovery defines they are α-1,4-glucan chains, likely consisting of at least 8 glucosyl units, and ultimately deriving from glycogen the only α-glucan described in the animal kingdom. As our methodology systematically excludes glucan chains shorter than DP 8 from quantification we cannot rule out that human CSF also contains those. In diseases that are characterized

by an abnormal accumulation of brain glycogen, CSF α-glucan could serve as a biomarker. In particular in LD, where the accumulating insoluble glycogen is the driver of the disease, this biomarker might be a very direct readout for the efficacy of treatments that aim to reduce glycogen accumulation. However, a correlation of brain glycogen content and CSF α-glucan concentration has yet to be demonstrated.

Conclusions

Methodological advancements are described and employed, which will be relevant tools for the investigation of glycogen metabolism and related diseases. First, in mouse models of LD an inert (degradation resistant) fraction of glycogen has been demonstrated and quantified in skeletal muscle (5 months old) and hippocampus (3 months old) by the introduction of a simple pre-extraction incubation. The inert glycogen (or α-glucan) correlates with the presence of insoluble glycogen and can readily be detected when LD-related accumulation of insoluble glycogen is still very low and masked by biological variation of a comparatively high soluble glycogen amount, such as in young mice. Effective detection of molecular disease markers, such as the insoluble glycogen in LD, in young mice greatly facilitates

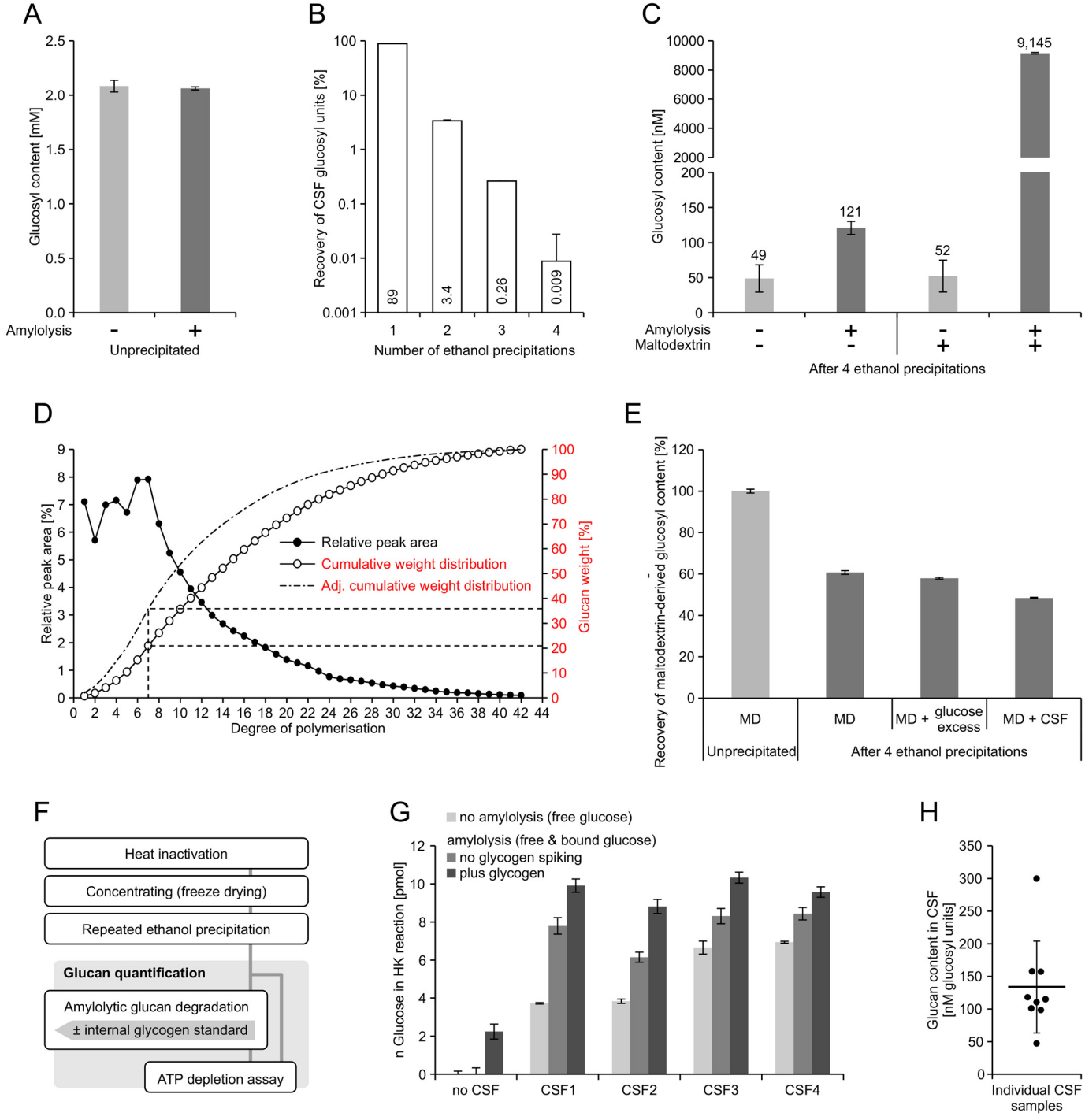

and accelerates pre-clinical research projects. Second, via the proxy of α-glucan, glycogen has been quantified in HEK293 cells using a medium-throughput assay. This enables reliable quantitative cell-based studies of glycogen synthesis, for instance with candidate inhibitors of glycogen synthase. Third, the high sensitivity glucose assay with detection of ATP depletion described in this work enabled detection of α-glucan using only a low number of cells and facilitated the discovery of minute amounts of α-glucan material in normal human CSF, establishing a novel methodological platform for biomarker analyses in GSDs, such as LD or APBD.

Experimental procedures

Mice, cells, materials

Mice of two LD models, *Epm2a*$^{-/-}$ (Epm2a$^{tm1.1Kzy}$, mixed C57BL/6 and 129Svj genetic background (51)) and *Epm2b*$^{-/-}$ (Nhlrc1^{tm1Bmin}, mixed C57BL/6Ncr and 129S6/SvEvTac genetic background (52)), respectively, have been previously described. Male WT and mutant mice were littermates from heterozygous breedings, housed with environmental enrichment in ventilated cages at 20-22°C and fed a commercially available diet with water accessible *ad libitum*. Healthy animals that did not undergo any previous procedure or treatment were sacrificed by cervical dislocation. The hind limb muscle as well as the brain after sagittal separation of the hemispheres and dissection of the hippocampi were immediately frozen in liquid nitrogen and stored at −80 °C until further use. All animal procedures were approved by The Centre for Phenogenomics Animal Care Committee and are in compliance with the Canadian Council for Animal Care Guidelines and the OMAFRA Animals for Research Act. HEK293FT cells (female human embryonic kidney) were cultured in DMEM containing 10% (v/v) FBS, 100 units/ml of penicillin, and 100 mg/ml of streptomycin, unless otherwise stated, being maintained at 37 °C in a humidified 5% CO_2 incubator. Human CSF from individuals without disease indication was obtained from BioIVT, LCC. CSF was stored at −80 °C until further use. Other materials and reagents, such as hexokinase (Roche, 11426362001), glucose-6-phosphate dehydrogenase (Roche, 1016587001), NADP (Roche, 10128058001), ATP (Roche, 10127523001), amyloglucosidase (Megazyme, E-AMGDF; Sigma, A1602), ATP-detection kit (Thermo Fisher Scientific, A22066), maltodextrin (Sigma, 419672), rabbit liver glycogen (Sigma, G8876), protein assay kit (Bio-Rad, 5000112), Bead Ruptor homogenization tubes ("BR-tubes," OMNI International, 19-648), Bead Ruptor ceramic beads ("BR-beads," OMNI International, 19-646), 96-well PCR plates (Bio-Rad, MLL9601), 8-strip caps (NEST, 406011), white 96-well half-area microplates (Sigma, CLS3693), poly-D-lysine (Sigma P0899), and DMEM without glucose and sodium pyruvate (Thermo Fisher Scientific 11966025) were obtained from the indicated vendor under given catalogue number.

Quantification of total and inert glycogen in mouse skeletal muscle

Aliquots of 30-50 mg of frozen ground skeletal muscle were prepared and their exact weight determined. For quantification of inert glycogen a pre-extraction incubation was conducted at 37 °C in a hybridization oven for 1.5 h or for the indicated time before samples were frozen at −80 °C until further processing. Total glycogen was quantified without any pre-extraction incubation. Glycogen was extracted and quantified largely as previously published (23). After the addition of 300 μl of 30% (w/v) potassium hydroxide to the frozen tissue and vigorous mixing, the sample was incubated at 95 °C for 1 h with intermittent vortexing, prior to cooling to room temperature, the addition of 50 μl of 0.4 M sodium sulfate, subsequent mixing and the addition of 950 μl of 100% ethanol. The sample was mixed again and left precipitating overnight at −30 °C. Following centrifugation at 16,000 × *g* and 4 °C for 25 min and discarding of the supernatant, the glycogen underwent 3 rounds of re-dissolving (350 μl of water at 95 °C for 10 min with intermittent mixing, followed by cooling to room temperature), precipitation (67% ethanol, 15 mM LiCl at −30 °C, overnight), centrifugation as above, and discarding of the supernatant. Subsequently the glycogen pellet was dried at 70 °C and re-dissolved in water as above. The volume of water added to the dry pellet as well as that of re-dissolved sample added to the subsequent enzymatic hydrolysis reaction (in 100 μl, 100 mM sodium acetate buffer, pH 4.5, 1.63 units of amyloglucosidase (Megazyme), 1 h at 55 °C) were 350 and 15 μl, respectively, when total muscle glycogen was

Figure 3. Detection of α-glucans in human CSF. *A,* glucose concentrations determined with and without amylolytic treatment of a heat-denatured and concentrated sample of pooled human CSF. Averages and mean absolute deviations (*error bars*) of two technical replicates are shown. *B,* recovery of total glucosyl units in the supernatants of four consecutive precipitations of a heat-denatured and concentrated sample of pooled human CSF in 90% ethanol. Values represent percentages as compared with total glucosyl content in the unprecipitated sample shown in *A*, *e.g.* during the first precipitation 89% of total glucosyl units in the sample were recovered in the ethanolic supernatant. Averages and mean absolute deviation (*error bars*) of two technical replicates are shown. *C,* glucose concentrations determined with and without amylolytic treatment of a heat-denatured and concentrated sample of pooled human CSF that underwent four rounds of precipitation in 90% ethanol, either in the absence or presence of an authentic maltodextrin standard. Averages and mean absolute deviations (*error bars*) of two technical replicates are shown. *D,* representative distributions of chain length (degree of polymerization *versus* relative peak area, *left axis*) and of cumulative weight (*right axis*) of the maltodextrin standard used in *C*. The elimination of chains with seven or less glucosyl units during repeated precipitation is expected to reduce maltodextrin recovery by at least 20% if the cumulative weight distribution is calculated based on the assumption that each chain length is detected with similar molar sensitivity. However, shorter chains detected less sensitively and are usually underrepresented. An adjusted cumulative weight distribution according to the model of Koch *et al*. (50) predicts a loss of around 36%. *E,* recovery of authentic MD after four consecutive 90% ethanol precipitations in the absence or presence of an excess of authentic glucose or of pooled human CSF. Before the precipitations authentic glucose and glucose in human CSF was in 260- and 110-fold excess of maltodextrin-derived glucose, respectively. Averages and mean absolute deviations (*error bars*) of two technical replicates are shown. *F,* schematic illustrating the procedure for the determination of α-glucans in CSF using the sensitive ATP depletion assay for glucose quantification. Results displayed in *G* and *H* were obtained using this procedure. *G,* amylolytical treatment releases glucose from human CSF. Heat-inactivated, concentrated, and precipitated human CSF (see *F*) was subjected to glucose quantification using an ATP depletion assay with or without prior amylolytic treatment in the presence or absence of an internal standard of commercial glycogen. Averages and mean absolute deviation (*error bars*) of two technical replicates for four individual CSF samples and "no CSF" controls are displayed. Detected glucose content is expressed as glucose amount in the HK reaction of the glucose assay with ATP-depletion detection (see Fig. 2*A*). *H,* average glucan content and standard deviation over nine individual human CSF samples, each determined as the difference of glucose detected with and without prior amylolytic treatment (shown in *G* for four samples).

quantified. The volumes were adjusted to allow reliable detection in the following glucose assay when samples with low glycogen contents were processed. After centrifugation (room temperature, 16,000 × *g*, 20 min), glucose levels were determined in supernatants of the hydrolysates as well as in seven serially diluted D-glucose standards using a previously reported method (53) performed in the 96-well format exactly as recently described (12). Glycogen content is given as glucose residues per gram fresh weight.

Quantification of inert α-glucans in mouse hippocampus

Intact and deep-frozen hippocampi were transferred to weighed and liquid nitrogen-cooled BR tubes. Tubes were incubated at room temperature for 30 or 60 min before being frozen at −80 °C until glycogen extraction. 20 min into the room temperature incubation the tissue weight was determined avoiding interference by condensation water. For glycogen extraction per tube 6 BR beads and 440 μl of cold 50 mM sodium acetate, pH 4.5, were added on ice, prior to securing the tightened cap with Parafilm and homogenization with a Bead Ruptor 24 located in a cold room (4 °C, program: 6 m/s, 2 cycles, 15 s/cycle, 5 s break). After a quick spin (15 s, 4 °C, 500 × *g*) and pellet resuspension by gentle vortexing, the homogenate was transferred into a fresh tube and heat-inactivated (15 min, 95 °C) before cooling to room temperature. Subsequently 180 μl of the homogenate were used for both enzymatic α-glucan hydrolysis (adding 1.63 units of amyloglucosidase (Megazyme) in 10 μl of 50 mM sodium acetate, pH 4.5, 1 h 55 °C) and a hydrolysis control (adding 10 μl of 50 mM sodium acetate, pH 4.5, 1 h on ice). Glucose was determined in 85 μl of hydrolysates and controls (each in duplicates) by a slightly modified version of a previously published method (12, 53): glucose standards were prepared in 50 mM sodium acetate buffer, pH 4.5, and both samples and standards were mixed with 150 μl of G6PDH reaction mix (150 μl of 200 mM Tricine/KOH, pH 8, 10 mM $MgCl_2$; 1 μl of 112.5 mM NADP; 1 μl of 180 mM of ATP; 0.5 units of G6PDH). After recording the background absorbance at 340 nm, 4 μl of HK (0.75 units in 4 μl of 200 mM Tricine/KOH, pH 8, 10 mM $MgCl_2$) were added and the absorbance was recorded again before calculation of glucose concentrations as previously described (12). Hippocampus glycogen was measured as α-glucan, *i.e.* the difference between glucose units measured in enzymatic hydrolysates (free and α-glucan-bound glucose) and hydrolysis controls (free glucose), and normalized to fresh weight.

Glucose quantification using an ATP depletion assay

In sealed 96-well PCR plates glucose standards and samples were subjected to HK reaction in 12 μl total volume containing 10 mM Tris, pH 7.5, 5 mM $MgCl_2$, 0.36 units HK, and an amount of ATP that exceeds that of the highest glucose standard by about 20%, such as 180 pmol of ATP when the highest glucose standard contains 144 pmol/reaction. The reaction was allowed to run for 45 min at room temperature. Meanwhile the "standard reaction solution" of a commercial ATP-detection kit (see above) was prepared as described in the manufacturer's instructions. The complete solution was protected from light and left to equilibrate to room temperature. The HK reaction mixtures were diluted by adding 108 μl of water with careful mixing prior to transferring 10 μl of the diluted HK reactions to a white 96-well half-area microplate, which subsequently received 90 μl of the standard reaction solution for ATP detection. The white plate was covered with aluminum foil, mixed for 2 min on a plate shaker at 600 rpm. Luminescence was detected after 15 min at 570 nm using a SpectraMax microplate luminescence reader with 750-ms signal integration time. This assay format was used for α-glucan determination in cell lysates (see below). It was adjusted as follows when used for the detection of α-glucans in human CSF: 1) HK reaction (14 μl of total volume, 22.8 mM Tricine, pH 8, 1.1 mM $MgCl_2$, 0.18 units of HK, 13 pmol of ATP for detecting maximal 10 pmol of glucose, 1 h incubation), and 2) 50 μl of water for HK reaction dilution.

Quantification of α-glucans from HEK293 cells

96-Well cell culture plates were coated with poly-D-lysine by 30 min incubation at room temperature with 200 μl/cm^2 of 10 μg/ml poly-D-lysine in PBS, followed by poly-D-lysine removal, washing with PBS, and air-drying of the plates. One day after seeding the cells at a density of 2-3 × 10^4 cells/well, cells were washed with PBS, and regular medium was replaced either by starvation medium (DMEM without glucose and sodium pyruvate, 5% FBS) or by fresh regular medium (for the nonstarved group). 24 h later, re-feeding began by changing back to regular medium with 5% FBS. After the indicated times cells were harvested in a cold room (4 °C).

The medium was removed, followed by washing the cells three to four times with PBS+ (containing 1 mM $CaCl_2$ and 1 mM $MgSO_4$). After removing PBS+, 80 μl of water were added. The cells were detached and resuspended using a multi-channel pipette, the cell suspension subsequently being split into different 96-well PCR plates for glycogen (45 μl) and protein quantification (18 μl) and in sealed plates were stored at −20 °C until further analysis.

For protein determination 4 μl of concentrated lysis buffer were added to 18 μl of cell suspension (samples) or water (blank) reaching a final concentration of 150 mM NaCl, 20 mM Tris, 12.1 mM deoxycholate, 1% Triton X-100, 0.1% SDS. Protein extraction was performed on a PCR block set to 4 °C. Samples were thawed, spun down (4 °C, 2000 × *g*, 3 min), and mixed by pipetting. The plate was tightly sealed, incubated (4 °C, 7.5 min), vortexed, and spun down (4 °C, 2000 × *g*, 1 min), followed by another round of incubation (see above) and vortexing. After centrifugation (4 °C, 2000 × *g*, 10 min), protein was quantified in supernatants using the Bio-Rad DC protein assay according to the manufacturer's protocol with calibration against BSA standard solutions.

For glycogen content analysis samples were thawed at 4 °C on a PCR block, spun down (4 °C, 2000 × *g*, 3 min), and incubated at 95 °C for 80 min, with one intermittent cycle of vortexing and spinning down. Air-tightness of the plate was achieved by using 8-strip caps, by applying pressure on the lid, and cooling down first to at least 50 °C before opening the PCR machine. After heat treatment, samples were collected by centrifugation (room temperature, 2000 × *g*, 3 min) and the pH adjusted to pH 4-5 by adding 5 μl of 100 mM sodium acetate buffer, pH 4.7.

3.97 μl of amyloglucosidase (Sigma) solution (2.17 milliunits/μl) or water (nonamylolysis controls) was added to aliquots (22.5 μl) of well-resuspended sample. Amylolysis was conducted at 55 °C overnight, whereas controls were stored at −20 °C. Subsequently, to both a mixture of Tris buffer, pH 7.5, and 0.5 M KOH was used to adjust the pH to 7.5 at 20 mM final concentration of Tris. Of the final volume (30.77 μl), 6 μl were used alongside glucose standard solutions for glucose quantification using an ATP depletion (described above). The glucan content as normalized to total protein content of the cells (protein-based glucan content) was calculated as the difference of glucose amounts per well determined with and without amylolysis and division by protein content per well.

Determination of α-glucans in human cerebrospinal fluid

Frozen commercial normal human CSF was directly subjected to heat denaturing for 15 min at 95 °C in the original sample tube. Subsequently a defined volume (around 1 ml) of CSF was transferred to fresh tubes and freeze-dried overnight. After that several samples were dissolved in water and pooled for initial experiments as described, later CSF samples were treated separately. Aliquots of pooled and ≈17-fold concentrated CSF were subjected to glucose assay (as previously described (12)) with and without prior amylolysis (in 100 μl of 100 mM sodium acetate, pH 4.5, with or without 1.63 unit of amyloglucosidase, Megazyme), each before (using 4 μl of concentrated and pooled CSF) and after (using 117 μl of concentrated and pooled CSF) several rounds of ethanol precipitation (1 h rotating, 4 °C, 90% ethanol, 20 mM NaCl) either in the presence or absence of an oligo-maltodextrin (MD) standard (42.75 nmol of Glc residues). The same amount of MD was subjected to identical precipitation conditions in the absence of CSF, as well as in the presence of 11.2 μM authentic glucose. After each precipitation samples were centrifuged (20 min, 16,000 × *g*, 4 °C), the supernatant was collected in fresh tubes, and the pellet dissolved in water. The supernatant was dried (vacuum centrifuge), re-dissolved in water, and aliquots were subjected to glucose quantification with and without prior amylolysis (as above).

Freeze-dried individual CSF samples were resuspended in 50 μl of 200 mM NaCl and heated for 10 min at 95 °C with intermittent vortexing before being cooled to room temperature. After a short spin 500 μl of 100% ethanol was added followed by vigorous mixing and the samples were left to precipitate for >1 h at 4 °C on a rotator and subsequent centrifugation (4 °C, 20 min, 16,000 × *g*) with discarding of the supernatant. Subsequently three rounds of the following steps were conducted: 1) resuspension of the pellet (50 μl of water, 5 min 95 °C), 2) precipitation by adding 450 μl of 100% ethanol (for 1 h, 4 °C), and 3) centrifugation (as described above) removal of the supernatant. The pellet was then dried in a vacuum centrifuge and resuspended in 65 μl of 20 mM NaOAc, pH 4, by vortexing thoroughly. If necessary, the pH was adjusted to 4-5 by the addition of defined volumes of dilute HCl. 5 μl of the sample were used for amylolysis (overnight at 55 °C in 30 μl total volume: 2 milliunits of amyloglucosidase (Sigma), 20 mM NaOAc, pH 4.5, with or without spiking by commercial rabbit liver glycogen as internal digestion control) and amylolysis control (as amylolysis except overnight at −20 °C without amyloglucosidase), both being treated alongside CSF-free controls. 6 μl of hydrolysates and controls were used for glucose quantification using the ATP depletion assay described above. CSF α-glucan content was calculated from the difference between glucose contents with and without amylolysis after correcting all glucose contents for the amount of glucose found in the "no CSF" controls.

Chain length distribution

20 μg of commercial oligo-maltodextrin was applied to HPAEC-PAD (Thermo Fisher, ICS5000). Oligoglucan chains were separated as described previously (23) and chromatograms were analyzed with Dionex Chromeleon 7.2. The relative peak areas for each chain length (DP) were determined. A cumulative relative weight distribution, which assumes equal detection of all chain lengths, was calculated by multiplying the relative peak area (RA) of each DP with the DP, followed by normalization to 100% for $\sum RA_n \times DP_n$, and addition of these normalized weighted relative areas for DP_1 to DP_n. An adjusted cumulative weight distribution was calculated after dividing RA_n by $((85.26/DP_n) + 16.15)$ according to the model of Koch *et al.* (50), which takes into account different detector responses at different chain lengths. Adjusted RA_n were normalized to 100% for $\sum RA_n$ and added for DP_1 to DP_n At least 5 technical replicates were analyzed, a representative shown.

Statistical analyses

Biological replicates were as indicated for analyses (*a*) in mouse skeletal muscle $n = 6$, (*b*) in mouse hippocampus $n = 2$, (*c*) in cell-based experiments $n = 7$-8, (*d*) in human CSF $n = 9$. If averages were calculated, standard deviation (S.D.) was used. When averages of two technical replicates were calculated the mean absolute deviation (MAD; $|x_1 - x_2x|/2$) is displayed. Upon calculation of differences between two independently determined quantities MAD was adjusted by calculating the square root of the sum of the square of both independent MADs. Statistical comparison of two groups has been performed by Welch's unpaired two-tailed *t* test. Multiple groups have been compared by one-way analysis of variance and Tukey post hoc tests. To determine whether α-glucan concentrations in human CSF are greater than 0, a Kolmogorov-Smirnov test for normality was performed, which was followed by a two-tailed one sample *t* test if the former test was passed. Statistical testing was performed using GraphPad Prism 8.

Data availability

All data referred to is included in this paper.

Acknowledgments—We thank Michael Emes and Ian Tetlow (University of Guelph, Canada) for facilitating the use of the HPAEC-PAD equipment, and Roman Melnyk (The Hospital for Sick Children, Toronto, Canada) for making his luminescence reader available for this study.

Author contributions—S. N., B. A. M., and F. N. conceptualization; S. N. and F. N. data curation; S. N., S. P., and F. N. formal analysis;

S. N. and F. N. validation; S. N., S. P., S. A., and F. N. investigation; S. N. and F. N. visualization; S. N., S. A., and F. N. methodology; S. N. project administration; S. N., S. P., S. A., B. A. M., and F. N. writing-review and editing; B. A. M. and F. N. funding acquisition; F. N. supervision; F. N. writing-original draft.

Funding and additional information—This work was supported by the Chelsea's Hope Lafora Disease Research Fund, Associazione Italiana Lafora (AILA), France-Lafora, the Milana and Tatjana Gajic Lafora Disease Foundation, Genome Canada, the Ontario Brain Institute (OBI), and National Institutes of Health NIDDS Grant P01 NS097197 (to S. N., S. A., B. A. M. and F. N.), and a University of Texas Southwestern Jimmy Elizabeth Westcott Distinguished Chair in Pediatric Neurology (to B. A. M.). The content is solely the responsibility of the authors and does not necessarily represent the official views of the National Institutes of Health.

Conflict of interest—The authors declare that they have no conflicts of interest with the contents of this article.

Abbreviations—The abbreviations used are: GSD, glycogen storage disease; LD, Lafora disease; CSF, cerebrospinal fluid; PAS, periodic acid-Schiff; G6PDH, glucose-6-phosphate dehydrogenase; HK, hexokinase; DP, degree of polymerization; HPAEC-PAD, high performance anion exchange chromatography with pulsed amperometric detection; DMEM, Dulbecco's modified Eagle's medium; FBS, fetal bovine serum; Tricine, *N*-[2-hydroxy-1,1-bis(hydroxymethyl)ethyl]glycine; MD, maltodextrin; RA, relative area; MAD, mean absolute deviation.

References

1. Roach, P. J., Depaoli-Roach, A. A., Hurley, T. D., and Tagliabracci, V. S. (2012) Glycogen and its metabolism: some new developments and old themes. *Biochem. J.* **441,** 763–787 CrossRef Medline
2. Adeva-Andany, M. M., González-Lucán, M., Donapetry-García, C., Fernández-Fernández, C., and Ameneiros-Rodríguez, E. (2016) Glycogen metabolism in humans. *Biochim. Biophys. Acta* **5,** 85–100 CrossRef Medline
3. Testoni, G., Duran, J., García-Rocha, M., Vilaplana, F., Serrano, A. L., Sebastian, D., López-Soldado, I., Sullivan, M. A., Slebe, F., Vilaseca, M., Munoz-Cánoves, P., and Guinovart, J. J. (2017) Lack of glycogenin causes glycogen accumulation and muscle function impairment. *Cell Metab.* **26,** 256–266e254 CrossRef Medline
4. Gidley, M. J., and Bulpin, P. V. (1987) Crystallisation of malto-oligosaccharides as models of the crystalline forms of starch: minimum chain-length requirement for the formation of double helices. *Carbohydr. Res.* **161,** 291–300 CrossRef
5. Kanungo, S., Wells, K., Tribett, T., and El-Gharbawy, A. (2018) Glycogen metabolism and glycogen storage disorders. *Ann. Transl. Med.* **6,** 474 CrossRef Medline
6. Guerra, A. S., van Diggelen, O. P., Carneiro, F., Tsou, R. M., Simoes, S., and Santos, N. T. (1986) A juvenile variant of glycogenosis IV (Andersen disease). *Eur. J. Pediatr.* **145,** 179–181 CrossRef Medline
7. Lafora, G. R., and Glueck, B. (1911) Beitrag zur histopathologie der myoklonischen epilepsie. *Z. Gesamte Neurol. Psychiatr.* **6,** 1–14 CrossRef
8. Arad, M., Benson, D. W., Perez-Atayde, A. R., McKenna, W. J., Sparks, E. A., Kanter, R. J., McGarry, K., Seidman, J. G., and Seidman, C. E. (2002) Constitutively active AMP kinase mutations cause glycogen storage disease mimicking hypertrophic cardiomyopathy. *J. Clin. Investig.* **109,** 357–362 CrossRef
9. Hays, A. P., Hallett, M., Delfs, J., Morris, J., Sotrel, A., Shevchuk, M. M., and DiMauro, S. (1981) Muscle phosphofructokinase deficiency: abnormal polysaccharide in a case of late-onset myopathy. *Neurology* **31,** 1077–1077 CrossRef Medline
10. Nitschke, F., Ahonen, S. J., Nitschke, S., Mitra, S., and Minassian, B. A. (2018) Lafora disease: from pathogenesis to treatment strategies. *Nat. Rev. Neurol.* **14,** 606–617 CrossRef
11. Navarro, P. P., Genoud, C., Castaño-Díez, D., Graff-Meyer, A., Lewis, A. J., de Gier, Y., Lauer, M. E., Britschgi, M., Bohrmann, B., Frank, S., Hench, J., Schweighauser, G., Rozemuller, A. J. M., van de Berg, W. D. J., Stahlberg, H., *et al.* (2018) Cerebral corpora amylacea are dense membranous labyrinths containing structurally preserved cell organelles. *Sci. Rep.* **8,** 18046 CrossRef Medline
12. Sullivan, M. A., Nitschke, S., Skwara, E. P., Wang, P., Zhao, X., Pan, X. S., Chown, E. E., Wang, T., Perri, A. M., Lee, J. P. Y., Vilaplana, F., Minassian, B. A., and Nitschke, F. (2019) Skeletal muscle glycogen chain length correlates with insolubility in mouse models of polyglucosan-associated neurodegenerative diseases. *Cell Rep.* **27,** 1334–1344 CrossRef Medline
13. Tang, B., Frasinyuk, M. S., Chikwana, V. M., Mahalingan, K. K., Morgan, C. A., Segvich, D. M., Bondarenko, S. P., Mrug, G. P., Wyrebek, P., Watt, D. S., DePaoli-Roach, A. A., Roach, P. J., and Hurley, T. D. (2020) Discovery and development of small-molecule inhibitors of glycogen synthase. *J. Med. Chem.* **63,** 3538–3551 CrossRef Medline
14. Thalia, T. R., and Peter, K. P. (2019) Cerebrospinal fluid biomarkers in neurodegenerative disorders. *Future Neurol.* **14,** FNL6 CrossRef
15. Hallgren, P., Hansson, G., Henriksson, K. G., Häger, A., Lundblad, A., and Svensson, S. (1974) Increased excretion of a glucose-containing tetrasaccharide in the urine of a patient with glycogen storage disease type II (Pompe's disease). *Eur. J. Clin. Invest.* **4,** 429–433 CrossRef
16. Piraud, M., Pettazzoni, M., de Antonio, M., Vianey-Saban, C., Froissart, R., Chabrol, B., Young, S., and Laforet, P., and French Pompe Study Group (2020) Urine glucose tetrasaccharide: a good biomarker for glycogenoses type II and III? a study of the French cohort. *Mol. Genet. Metab. Rep.* **23,** 100583–100583 CrossRef Medline
17. Minassian, B. A. (2001) Lafora's disease: towards a clinical, pathologic, and molecular synthesis. *Pediatr. Neurol.* **25,** 21–29 CrossRef
18. Baba, O. (1993) Production of monoclonal antibody that recognizes glycogen and its application for immunohistochemistry. *Kokubyo Gakkai Zasshi* **60,** 264–287 CrossRef
19. Skurat, A. V., Segvich, D. M., DePaoli-Roach, A. A., and Roach, P. J. (2017) Novel method for detection of glycogen in cells. *Glycobiology* **27,** 416–424 CrossRef Medline
20. Toki, M. I., Cecchi, F., Hembrough, T., Syrigos, K. N., and Rimm, D. L. (2017) Proof of the quantitative potential of immunofluorescence by mass spectrometry. *Lab. Invest.* **97,** 329–334 CrossRef Medline
21. Suzuki, Y., Lanner, C., Kim, J. H., Vilardo, P. G., Zhang, H., Yang, J., Cooper, L. D., Steele, M., Kennedy, A., Bock, C. B., Scrimgeour, A., Lawrence, J. C., and DePaoli-Roach, A. A. (2001) Insulin control of glycogen metabolism in knockout mice lacking the muscle-specific protein phosphatase PP1G/RGL. *Mol. Cell Biol.* **21,** 2683–2694 CrossRef Medline
22. Tagliabracci, V. S., Girard, J. M., Segvich, D., Meyer, C., Turnbull, J., Zhao, X., Minassian, B. A., DePaoli-Roach, A. A., and Roach, P. J. (2008) Abnormal metabolism of glycogen phosphate as a cause for Lafora disease. *J. Biol. Chem.* **283,** 33816–33825 CrossRef Medline
23. Nitschke, F., Sullivan, M. A., Wang, P., Zhao, X., Chown, E. E., Perri, A. M., Israelian, L., Juana-Lopez, L., Bovolenta, P., Rodriguez de Cordoba, S., Steup, M., and Minassian, B. A. (2017) Abnormal glycogen chain length pattern, not hyperphosphorylation, is critical in Lafora disease. *EMBO Mol. Med.* **9,** 906–917 CrossRef
24. Lomako, J., Lomako, W. M., Kirkman, B. R., and Whelan, W. J. (1994) The role of phosphate in muscle glycogen. *BioFactors* **4,** 167–171 Medline
25. Tagliabracci, V. S., Turnbull, J., Wang, W., Girard, J. M., Zhao, X., Skurat, A. V., Delgado-Escueta, A. V., Minassian, B. A., Depaoli-Roach, A. A., and Roach, P. J. (2007) Laforin is a glycogen phosphatase, deficiency of which leads to elevated phosphorylation of glycogen *in vivo*. *Proc. Natl. Acad. Sci. U.S.A.* **104,** 19262–19266 CrossRef Medline
26. Young, L. E. A., Brizzee, C. O., Macedo, J. K. A., Murphy, R. D., Contreras, C. J., DePaoli-Roach, A. A., Roach, P. J., Gentry, M. S., and Sun, R. C. (2020) Accurate and sensitive quantitation of glucose and glucose phosphates derived from storage carbohydrates by mass spectrometry. *Carbohydr. Polymers* **230,** 115651 CrossRef Medline

27. Parker, G. J., Koay, A., Gilbert-Wilson, R., Waddington, L. J., and Stapleton, D. (2007) AMP-activated protein kinase does not associate with glycogen α-particles from rat liver. *Biochem. Biophys. Res. Commun.* **362,** 811–815 CrossRef Medline
28. Gong, X., Wang, S., and Qu, H. (2011) Solid-liquid equilibria of D-glucose, D-fructose and sucrose in the mixture of ethanol and water from 273.2 K to 293.2 K. *Chinese J. Chem. Eng.* **19,** 217–222 CrossRef
29. Haebel, S., Hejazi, M., Frohberg, C., Heydenreich, M., and Ritte, G. (2008) Mass spectrometric quantification of the relative amounts of C6 and C3 position phosphorylated glucosyl residues in starch. *Anal. Biochem.* **379,** 73–79 CrossRef Medline
30. Nitschke, F., Wang, P., Schmieder, P., Girard, J.-M., Awrey, D. E., Wang, T., Israelian, J., Zhao, X., Turnbull, J., Heydenreich, M., Kleinpeter, E., Steup, M., and Minassian, B. A. (2013) Hyperphosphorylation of glucosyl C6 carbons and altered structure of glycogen in the neurodegenerative epilepsy Lafora disease. *Cell Metab.* **17,** 756–767 CrossRef Medline
31. Brewer, M. K., Uittenbogaard, A., Austin, G. L., Segvich, D. M., DePaoli-Roach, A., Roach, P. J., McCarthy, J. J., Simmons, Z. R., Brandon, J. A., Zhou, Z., Zeller, J., Young, L. E. A., Sun, R. C., Pauly, J. R., Aziz, N. M., *et al.* (2019) Targeting pathogenic Lafora bodies in Lafora disease using an antibody-enzyme fusion. *Cell Metab.* **30,** 689–705.e6 CrossRef
32. Balto, A. S., Lapis, T. J., Silver, R. K., Ferreira, A. J., Beaudry, C. M., Lim, J., and Penner, M. H. (2016) On the use of differential solubility in aqueous ethanol solutions to narrow the DP range of food-grade starch hydrolysis products. *Food Chem.* **197,** 872–880 CrossRef Medline
33. Sullivan, M. A., Aroney, S. T., Li, S., Warren, F. J., Joo, J. S., Mak, K. S., Stapleton, D. I., Bell-Anderson, K. S., and Gilbert, R. G. (2014) Changes in glycogen structure over feeding cycle sheds new light on blood-glucose control. *Biomacromolecules* **15,** 660–665 CrossRef Medline
34. Strehler, B. L., and Totter, J. R. (1952) Firefly luminescence in the study of energy transfer mechanisms: I. substrate and enzyme determination. *Arch. Biochem. Biophys.* **40,** 28–41 CrossRef
35. Petty, R. D., Sutherland, L. A., Hunter, E. M., and Cree, I. A. (1995) Comparison of MTT and ATP-based assays for the measurement of viable cell number. *J. Biolumin. Chemilumin.* **10,** 29–34 CrossRef Medline
36. Sykes, M. L., and Avery, V. M. (2009) A luciferase based viability assay for ATP detection in 384-well format for high throughput whole cell screening of *Trypanosoma brucei brucei* bloodstream form strain 427. *Parasit. Vectors* **2,** 54 CrossRef Medline
37. DePaoli-Roach, A. A., Tagliabracci, V. S., Segvich, D. M., Meyer, C. M., Irimia, J. M., and Roach, P. J. (2010) Genetic depletion of the malin E3 ubiquitin ligase in mice leads to Lafora bodies and the accumulation of insoluble Laforin. *J. Biol. Chem.* **285,** 25372–25381 CrossRef Medline
38. Irimia, J. M., Tagliabracci, V. S., Meyer, C. M., Segvich, D. M., DePaoli-Roach, A. A., and Roach, P. J. (2015) Muscle glycogen remodeling and glycogen phosphate metabolism following exhaustive exercise of wild type and Laforin knockout mice. *J. Biol. Chem.* **290,** 22686–22698 CrossRef Medline
39. Ren, J. M., Gulve, E. A., Cartee, G. D., and Holloszy, J. O. (1992) Hypoxia causes glycogenolysis without an increase in percent phosphorylase a in rat skeletal muscle. *Am. J. Physiol.* **263,** E1086–1091 CrossRef
40. Cohen, N., Rossetti, L., Shlimovich, P., Halberstam, M., Hu, M., and Shamoon, H. (1995) Counterregulation of hypoglycemia: skeletal muscle glycogen metabolism during three hours of physiological hyperinsulinemia in humans. *Diabetes* **44,** 423–430 CrossRef
41. Kakhlon, O., Ferreira, I., Solmesky, L. J., Khazanov, N., Lossos, A., Alvarez, R., Yetil, D., Pampou, S., Weil, M., Senderowitz, H., Escriba, P., Yue, W. W., and Akman, H. O. (2018) Guaiacol as a drug candidate for treating adult polyglucosan body disease. *JCI Insight* **3,** CrossRef
42. Bergmeyer, H. U. (1975) New values for the molar extinction coefficients of NADH and NADPH for the use in routine laboratories (author's transl). *Z. Klin. Chem. Klin. Biochem.* **13,** 507–508 Medline
43. Turnbull, J., DePaoli-Roach, A. A., Zhao, X., Cortez, M. A., Pencea, N., Tiberia, E., Piliguian, M., Roach, P. J., Wang, P., Ackerley, C. A., and Minassian, B. A. (2011) PTG depletion removes Lafora bodies and rescues the fatal epilepsy of Lafora disease. *PLoS Genet.* **7,** e1002037 CrossRef Medline
44. Turnbull, J., Epp, J. R., Goldsmith, D., Zhao, X., Pencea, N., Wang, P., Frankland, P. W., Ackerley, C. A., and Minassian, B. A. (2014) PTG protein depletion rescues malin-deficient Lafora disease in mouse. *Ann. Neurol.* **75,** 442–446 CrossRef Medline
45. Lahiri, V. L. (1973) Amylase activity of cerebrospinal fluid and serum in neurological disorders. *Indian J. Pediatr.* **40,** 217–219 CrossRef Medline
46. Leen, W. G., Willemsen, M. L A., Wevers, R. A., and Verbeek, M. M. (2012) Cerebrospinal fluid glucose and lactate: age-specific reference values and implications for clinical practice. *PLoS ONE* **7,** e42745–e42745 CrossRef Medline
47. Good, C. A., Kramer, H., and Somogyi, M. (1933) *J. Biol. Chem.* **100,** 485–491
48. Manners, D. J. (1991) Recent developments in our understanding of glycogen structure. *Carbohydr. Polymers* **16,** 37–82 CrossRef
49. Koizumi, K., Fukuda, M., and Hizukuri, S. (1991) Estimation of the distributions of chain length of amylopectins by high-performance liquid chromatography with pulsed amperometric detection. *J. Chromatogr. A* **585,** 233–238 CrossRef
50. Koch, K., Andersson, R., and Åman, P. (1998) Quantitative analysis of amylopectin unit chains by means of high-performance anion-exchange chromatography with pulsed amperometric detection. *J. Chromatogr. A* **800,** 199–206 CrossRef
51. Ganesh, S., Delgado-Escueta, A. V., Sakamoto, T., Avila, M. R., Machado-Salas, J., Hoshii, Y., Akagi, T., Gomi, H., Suzuki, T., Amano, K., Agarwala, K. L., Hasegawa, Y., Bai, D. S., Ishihara, T., Hashikawa, T., *et al.* (2002) Targeted disruption of the *Epm2a* gene causes formation of Lafora inclusion bodies, neurodegeneration, ataxia, myoclonus epilepsy and impaired behavioral response in mice. *Hum. Mol. Genet.* **11,** 1251–1262 CrossRef Medline
52. Turnbull, J., Wang, P., Girard, J. M., Ruggieri, A., Wang, T. J., Draginov, A. G., Kameka, A. P., Pencea, N., Zhao, X., Ackerley, C. A., and Minassian, B. A. (2010) Glycogen hyperphosphorylation underlies Lafora body formation. *Ann. Neurol.* **68,** 925–933 CrossRef Medline
53. Lowry, O. H. and Passonneau, J. V. (eds) (1972) *A flexible system of enzymatic analysis*. Academic Press, New York